Observation of Long-Wavelength Interface Phonons in a GaAs/AlGaAs Superlattice

Ph. Lambin,[a] J. P. Vigneron, A. A. Lucas, P. A. Thiry, M. Liehr,[b] J. J. Pireaux,[a] and R. Caudano
Institute for Research in Interface Sciences, Facultés Universitaires Notre-Dame de la Paix, B-5000 Namur, Belgium

and

T. J. Kuech
IBM Thomas J. Watson Research Center, Yorktown Heights, New York 10598
(Received 5 December 1985)

We report on the first observation of long-wavelength interface optical phonons in a GaAs/AlGaAs superlattice by high-resolution electron-energy-loss spectroscopy. The observed spectrum is well accounted for by scattering theory with material data taken from infrared spectroscopy.

PACS numbers: 73.40.Lq, 63.20.Dj, 79.20.Kz

There is currently intense interest in applying surface- and interface-sensitive techniques to the study of electron and phonon excitations in semiconductor superlattices.[1] Raman spectroscopy has recently been successfully used[2] to investigate bulk optical phonons "confined" to individual layers of a GaAs/AlAs superlattice as well as interface delocalized optical phonons of the same material.

In this Letter we present the first observation, by means of high-resolution electron-energy-loss spectroscopy (HREELS), of localized and delocalized interface optical phonons in a GaAs/$Al_{0.3}Ga_{0.7}As$ superlattice such as used for optoelectronic devices. HREELS, although primarily sensitive to surface vibrations, is thereby demonstrated to be also capable of probing interface phonons propagating throughout a semiconductor superlattice. In addition, we provide in this Letter an analysis of our observations in terms of a recently developed[3] theory of the inelastic scattering of electrons by the surface and interface optical phonons of a stratified medium. While this theory has already been applied for illustration purposes to idealized GaSb/AlSb and GaSb/InAs superlattices,[3] the present work is aimed at a quantitative interpretation of the highly resolved experimental spectrum of Fig. 1, devoted to a heterostructure of great current interest.

Our sample superlattice consists of 25 periods of alternate GaAs and $Al_{0.3}Ga_{0.7}As$ layers 100 ± 10 Å thick. The layers were grown on a ⟨100⟩-oriented GaAs substrate by metalorganic vapor phase epitaxy. The sample, exposing a GaAs layer at its surface, was stored in air before its introduction in the UHV chamber of the HREELS spectrometer. The unavoidable surface contaminants (mainly hydrocarbons and oxygen) were readily detected by their characteristic vibrational energy losses and could not be removed by heat treatment. A clean surface was obtained by argon-ion bombardment (0.5 keV, 5 $\mu A/cm^2$) during a time (10 min) kept at a minimum to avoid excessive surface damage. Under these conditions, it is estimated that 20 ± 10 Å had been removed by sputtering from the first GaAs layer. The sample was annealed at 300 °C for 30 min before the spectrum of Fig. 1 was recorded at room temperature (data points). The spectrum was measured in the specular direction with a primary electron energy of 5.6 eV, an angle of incidence of 45°, and a spectrometer aperture of 1.8°. On the right-hand side of the elastic peak, one distinguishes a main energy-loss peak at 292 cm^{-1} (peak A) and, appearing as a shoulder in the high-energy tail of this peak, there is a less intense but clearly distinct structure centered around 370 cm^{-1} (peak B). The corresponding gain peaks can be recognized symmetrically placed on the left-hand side of the elastic peak. Weak features could

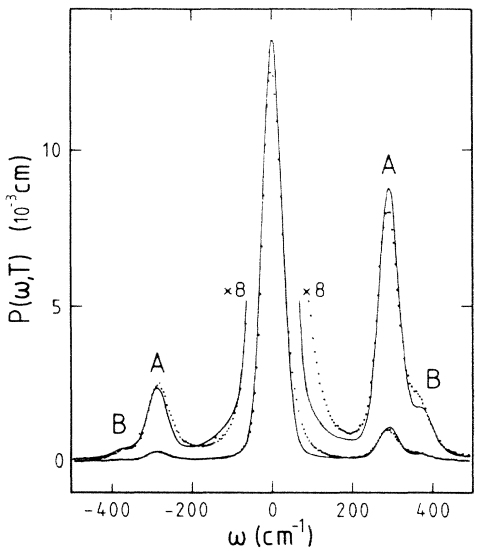

FIG. 1. Energy-loss probability for a GaAs/$Al_{0.3}Ga_{0.7}As$ [(100 Å)/(100 Å)] superlattice (dots) compared with the theoretical spectrum (full line) in reflection geometry (electron energy 5.6 eV, incidence angle 45°, surface temperature 300 K). In the simulated spectrum, the thickness of the topmost GaAs layer is reduced to 70 Å to account for the effect of sputter cleaning.

also be observed at energies corresponding to overtones or combination bands of peaks A and B (not shown in Fig. 1).

The energy distribution of electrons backscattered near the specular direction from the surface of polar materials is dominated, in the infrared range, by losses arising from the excitation of long-wavelength surface and interface optical vibrations. These vibrations, such as the phonons first described by Fuchs and Kliewer in an ionic slab,[4] result from long-range Coulomb interactions between ions in the target. The probability $P(\omega,T)d\omega$ that the backscattered electron transfers energy $\hbar\omega$ to the target at temperature T can be related to the classical spectrum $P_{\rm cl}(\omega)$ of the dielectric theory through the Fourier transform[3,5]

$$P(\omega,T)=(1/2\pi)\int_{-\infty}^{+\infty}F(t,T)e^{i\omega t}\,dt, \tag{1}$$

$$F(t,T)=\exp\{-\int_0^\infty P_{\rm cl}(\omega)[1-\cos(\omega t)]\coth(\hbar\omega/2k_BT)\,d\omega - i\int_0^\infty P_{\rm cl}(\omega)\sin(\omega t)\,d\omega\}. \tag{2}$$

When retardation effects are neglected, the classical spectrum $P_{\rm cl}(\omega)$ [the first moment of which, $\int_0^\infty \hbar\omega P_{\rm cl}(\omega)\,d\omega$, gives the average energy loss] is given by

$$P_{\rm cl}(\omega)=\frac{4e^2}{\pi^2\hbar}\int_D d^2k\,k\left[\frac{v_\perp}{(kv_\perp)^2+(\mathbf{k}\cdot\mathbf{v}_{\|}-\omega)^2}\right]^2 \mathrm{Im}\left[\frac{-1}{\xi(\mathbf{k},\omega)+1}\right]. \tag{3}$$

In (3), $\mathbf{k}$ is the emitted-phonon wave vector parallel to the surface of the target and D denotes a small elliptical integration domain[3] that depends on the angle of incidence and on the small circular aperture of the spectrometer which, through energy and momentum conservation, rejects electrons with momentum transfer $\mathbf{k}$ outside D. $\mathbf{v}_{\|}$ and $v_\perp$ are the electron velocity components with respect to the surface and ξ is the dielectric response function of the target.

For interpretation of the data of Fig. 1, it is important to note that, in HREELS, only the surface response function, $\mathrm{Im}[-1/(\xi+1)]$, and not the bulk one, $\mathrm{Im}(-1/\epsilon)$, is relevant. This is because bulk phonons can be excited only when the probe electrons penetrate deeply into the target. Indeed, contrary to surface and interface phonons, bulk vibrations have vanishing electric fields in vacuum, beyond a microscopic neighborhood of the surface, and hence cannot be excited by an electron that does not penetrate deeply below the surface of the target.[6]

On account of the smallness of the allowed values of $\mathbf{k}$, ξ can be deduced from the Maxwell equations governing the macroscopic electric field of the long-wavelength vibrations in the target. For a target made of isotropic layers separated by sharp neutral interfaces, ξ can be expressed as the continued fraction[3]

$$\xi(\mathbf{k},\omega)=a_1-\cfrac{b_1^2}{a_1+a_2-\cfrac{b_2^2}{a_2+a_3-\ldots}}, \tag{4}$$

with[7] $a_i=\epsilon_i(\omega)/\tanh(kd_i)$ and $b_i=\epsilon_i(\omega)/\sinh(kd_i)$, where ϵ_i is the homogeneous dielectric constant of the ith layer of thickness d_i. In polar semiconductors, the bulk dielectric properties in the infrared range are well described by

$$\epsilon(\omega)=\epsilon_\infty+\sum_{j=1}^{n}\frac{Q_j\omega_{{\rm TO},j}^2}{\omega_{{\rm TO},j}^2-\omega^2-i\gamma_j\omega}, \tag{5}$$

where n is the number of bulk transverse-optical modes of frequencies $\omega_{{\rm TO},j}$, dampings γ_j, and strengths Q_j. For a heterostructure having a finite number of layers, Eq. (4) is then a rational function of ω^2. If we neglect temporarily the γ_j, the real zeros of $\xi(\mathbf{k},\omega)+1$, i.e., the poles of the response function in Eq. (3), give the dispersion relations of the Fuchs-Kliewer–type phonon modes in the heterostructure. The number of modes increases linearly with the number of interfaces. In a model superlattice where the first two layers are repeated periodically, nearly all the Fuchs-Kliewer interface modes propagate throughout the lattice and their dispersion-relation curves accumulate in continuum regions[3] of the (ω,k) plane. However, a few modes give rise to isolated branches[3,8-10] which represent vibrations localized near the external surface of the superlattice. Mathematically, the continued fraction (4) becomes periodic and converges to that solution of the quadratic equation

$$(a_1+a_2)\xi^2-(\epsilon_1^2-\epsilon_2^2)\xi-(a_1\epsilon_2^2+a_2\epsilon_1^2)=0 \tag{6}$$

closest to its first approximant $a_1-b_1^2/(a_1+a_2)$. Within the propagating-mode continua of the (ω,k) plane, Eq. (6) has two complex-conjugate solutions, whereas along the isolated branches of the evanescent modes the solution of Eq. (6) remains $\xi=-1$.

Let us now apply these general results to our GaAs/$Al_{0.3}Ga_{0.7}As$ superlattice with $d_1=d_2=100$ Å. For the calculations, a single oscillator in Eq. (5) is sufficient for GaAs, whereas two oscillators are required to reproduce the bulk infrared properties of AlGaAs.[11,12] Table I lists the oscillator parameters deduced from reflectivity measurements. Figure 2 gives the calculated dispersion relations of the interface modes (for vanishing dampings). Corresponding to the three-oscillator model, there are three continua

TABLE I. Oscillator parameters used throughout this Letter.[a]

Compound	ϵ_∞	Q	ω_{TO} (cm^{-1})	ω_{LO} (cm^{-1})	γ/ω_{TO}
GaAs	10.9	2.03	269	293	0.009
$Al_{0.3}Ga_{0.7}As$	10.2	1.24	265	278	0.027
		0.93	361	379	0.030

[a]Reference 11.

denoted A, B, B′ of delocalized interface modes and one localized branch of evanescent mode. The boundaries of the continua at $k=0$ occur at the ω_{TO} and ω_{LO} values listed in Table I. The large-k limit of the localized branch converges to the Fuchs-Kliewer surface phonon of a semi-infinite GaAs crystal. The classical EELS spectrum of the superlattice (Fig. 3) as computed from Eq. (3) (including dampings) is easily understood on the basis of Fig. 2. The strong peak at $\omega=292$ cm^{-1} is due to the localized branch along which $\mathrm{Im}[-1/(\xi+1)]$ assumes large values. The width of the peak is due to both the dispersion and the damping of the localized branch. The shoulder appearing in the low-frequency wing of the peak is due to the continuum of GaAs-like modes in region A. The weaker peak denoted by B in the high-frequency range 350–390 cm^{-1} originates from the corresponding B continuum of AlAs-like modes in Fig. 2. Finally the B′ continuum of GaAs-derived modes makes a very small contribution to the classical spectrum on the low-energy tail of the major A peak. The calculated classical spectrum shown in Fig. 3 (full line) takes account of a reduction of the thickness of the topmost GaAs layer caused by the sputter cleaning of the sample. [The continued-fraction formulation of the effective dielectric function in Eq. (4) allows for an arbitrary succession of layer thicknesses.] The dashed line in Fig. 3 applies to a perfect superlattice with an undisturbed top layer.

In order to compare these theoretical predictions to the experimental spectrum in Fig. 1, multiple-scattering and temperature effects must be included, as prescribed in Eqs. (1) and (2). In addition, the quantum-mechanical spectrum of Eq. (1) must further be convoluted with the response function of the spectrometer in such a way as to reproduce the observed width of the elastic peak. A symmetrical broadening function was used to reproduce the experimental resolution (56 cm^{-1} FWHM). As seen in Fig. 1, that resolution was sufficient to allow a definite identification of the losses (and gains) arising from the excitation of propagating interface phonons (peak B). Note the quality of the overall agreement between theory and experiment for both the positions and intensities of the A and B features (the B′ feature is too weak to be detected in the low-energy tail of peak A). This good agreement was obtained only with allowance for a thinner topmost GaAs layer as shown in Fig. 3.

Let us emphasize that we did not attempt to fit the detailed asymmetrical line shape of the observed elastic peak. The use of an asymmetrical broadening function to better reproduce the experimental elastic line shape would clearly affect the calculated shapes of peaks A and B and bring them in better agreement with the observed data.

Finally, one should reemphasize that, although very close in frequencies to the bulk phonon, observed by resonant Raman scattering in GaAs/AlGaAs superlat-

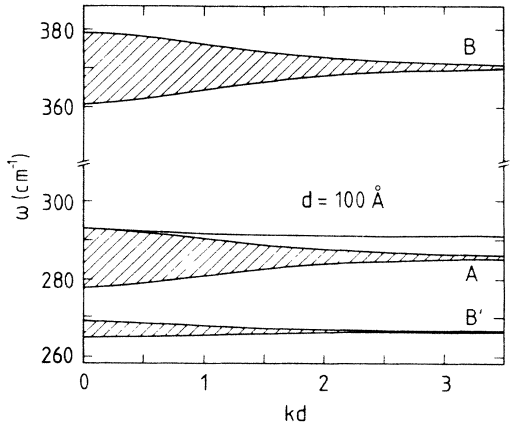

FIG. 2. Dispersion relations of Fuchs-Kliewer phonons in a semi-infinite $GaAs/Al_{0.3}Ga_{0.7}As$ superlattice when the thicknesses of both layers coincide ($d_1=d_2=d$).

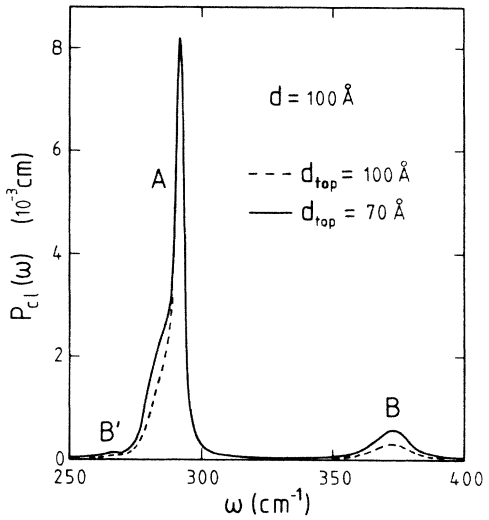

FIG. 3. Calculated classical energy-loss probability $P_{cl}(\omega)$ for a 5.6-eV electron (incidence angle 45°) specularly reflected at the surface of a $GaAs/Al_{0.3}Ga_{0.7}As$ [(100 Å)/(100 Å)] superlattice for the truly periodic superlattice (dashed line) and for the sputtered sample (full line). The labels A, B, and B′ refer to the ω regions shown in Fig. 2.

tices,[12] the spectral features of the loss spectrum in Fig. 1 are entirely due to surface and interface vibrations and not to bulk excitations which remain out of reach of HREELS in reflection geometry.

In conclusion, this Letter demonstrates the capability of EELS to assess optical surface- and interface-vibrational properties of multilayered semiconductor compounds. In combination with the dielectric theory, HREELS gives access to surface and interface optical constants, such as needed for instance to describe transport properties in two-dimensional electronic devices.

We acknowledge the financial support of the Belgian Fund for Joint Basic Research and the Belgian Ministry for Science Policy (IRIS project).

---

[a]Also at the Belgian Fonds National de la Recherche Scientifique.

[b]Present address: IBM Thomas J. Watson Research Center, P. O. Box 218, Yorktown Heights, N. Y. 10598.

[1]L. Esaki, J. Phys. (Paris), Colloq. **45**, C5-3 (1984).

[2]A. K. Sood, J. Menéndex, M. Cardona, and K. Ploog, Phys. Rev. Lett. **54**, 2111, 2115 (1985), and references therein.

[3]Ph. Lambin, J. P. Vigneron, and A. A. Lucas, Phys. Rev. B **32**, 8203 (1985).

[4]R. Fuchs and K. L. Kliewer, Phys. Rev. **140**, A2076 (1965).

[5]A. A. Lucas and M. Šunjić, Prog. Surf. Sci. **2**, 75 (1972); H. Raether, *Excitations of Plasmons and Interband Transitions by Electrons* (Springer-Verlag, Berlin, 1980); W. L. Schaich, Phys. Rev. B **24**, 686 (1981); H. Ibach and D. L. Mills, *Electron-Energy Loss Spectroscopy and Surface Vibrations* (Academic, New York, 1982).

[6]The vanishing of the external field results from a matching with the interior electric displacement $\epsilon\mathbf{E}$, with $\epsilon=0$ for *bulk* excitations. The electron penetration in HREELS can be estimated as 0.5 nm. Thus the electron–bulk-vibration interaction time is of order 5×10^{-16} s for 10-eV electrons, i.e., much too short as compared to a vibrational period of order 10^{-13} s. The quantitative evaluation of the bulk phonon excitation probability is given by A. A. Lucas, J. P. Vigneron, Ph. Lambin, P. A. Thiry, M. Liehr, J. J. Pireaux, and R. Caudano, in Proceedings of the Sanibel Island Symposium, St. Augustine, Florida, March 1985 [Int. J. Quantum Chem. (to be published)].

[7]When retardation effects need to be included, the proper coefficients to be used in Eq. (4) are $a_i=\epsilon_i/\alpha_i\tanh(k\alpha_i d_i)$ and $b_i=\epsilon_i/\alpha_i\sinh(k\alpha_i d_i)$, where $\alpha_i=(1-\epsilon_i\omega^2/k^2c^2)^{1/2}$ (unpublished work by the authors).

[8]E. P. Pokatilov and S. I. Beril, Phys. Status Solidi (b) **110**, K75 (1982).

[9]R. E. Camley and D. L. Mills, Phys. Rev. B **29**, 1695 (1984).

[10]G. F. Giuliani and J. J. Quinn, Phys. Rev. Lett. **51**, 919 (1983).

[11]O. K. Kim and W. G. Spitzer, J. Appl. Phys. **50**, 4362 (1979).

[12]J. E. Zucker, A. Pinczuk, D. S. Chemla, A. Gossard, and W. Wiegmann, Phys. Rev. B **29**, 7065 (1984).